

Theoretical Interpretation of the Measurements of the Secondary Eclipses of TrES-1 and HD209458b

A. Burrows¹, I. Hubeny¹, & D. Sudarsky¹

ABSTRACT

We calculate the planet-star flux-density ratios as a function of wavelength from 0.5 μm to 25 μm for the transiting extrasolar giant planets TrES-1 and HD209458b and compare them with the recent Spitzer/IRAC-MIPS secondary eclipse data in the 4.5, 8.0, and 24 μm bands. With only three data points and generic calibration issues, detailed conclusions are difficult, but inferences regarding atmospheric composition, temperature, and global circulation can be made. Our models reproduce the observations reasonably well, but not perfectly, and we speculate on the theoretical consequences of variations around our baseline models. One preliminary conclusion is that we may be seeing in the data indications that the day side of a close-in extrasolar giant planet is brighter in the mid-infrared than its night side, unlike Jupiter and Saturn. This correspondence will be further tested when the data anticipated in other Spitzer bands are acquired, and we make predictions for what those data may show.

Subject headings: stars: individual (TrES-1, HD209458)—(stars:) planetary systems—planets and satellites: general

1. Introduction

High-precision radial-velocity measurements of many nearby stellar primaries have revealed the presence of extrasolar giant planets (EGPs) in orbit around them (Mayor & Queloz 1995; Marcy & Butler 1996; Marcy & Butler 1998; Marcy, Cochran, & Major 2000, and references therein)¹. From these data, the projected mass ($M_p \sin(i)$, where M_p is the planet

¹Department of Astronomy and Steward Observatory, The University of Arizona, Tucson, AZ 85721; burrows@zenith.as.arizona.edu, hubeny@aegis.as.arizona.edu, sudarsky@as.arizona.edu

¹see J. Schneider's Extrasolar Planet Encyclopaedia at <http://www.obspm.fr/encycl/encycl.html> and the Carnegie/California compilation at <http://exoplanets.org> for a more-or-less up-to-date database of extrasolar planets and their primaries.

mass and i is the orbital inclination) and orbital parameters of more than 150 planetary companions have been determined. These data have revolutionized the study of planetary systems, not the least because their orbits and masses vary widely and are in general quite unlike those of our Jovian and ice giants.

The detection of a few transiting EGPs (currently seven), whose orbits are nearly edge-on, has provided radii, masses, and inclinations (Henry et al. 2000; Charbonneau et al. 2000; Brown et al. 2001; Sasselov 2003; Konacki et al. 2003ab; Konacki et al. 2004; Bouchy et al. 2004; Pont et al. 2004; Torres et al. 2005). For HD209458b, there are in addition indications of its atmospheric composition from the wavelength-dependence of the photometric dip of the stellar light during transit (Charbonneau et al. 2002; Vidal-Madjar et al. 2003; §2). Figure 1 depicts the mass-radius plot for these transiting EGPs, with Jupiter and Saturn themselves superposed.

However, it is only by direct detection of the planets and their photometric and spectroscopic characterization that they can be studied in depth to reveal their atmospheric and physical properties (Sudarsky, Burrows, & Hubeny 2003; Allard et al. 2003; Burrows, Sudarsky, & Hubeny 2004; Burrows 2005). While orbital distances (a), periods (P), and eccentricities (e) are reasonably well determined, the investigation of an EGP in physical detail requires at a minimum the actual mass (M_p), radius (R_p), and composition. Space provides the needed access, but it had generally been thought that high-contrast imaging is necessary to separate out the planet from the bright star. However, Charbonneau et al. (2005) and Deming et al. (2005) have recently shown that variations in the summed light of the planet and star for the close-in transiting EGPs TrES-1 and HD209458b can be detected with Spitzer during secondary eclipse. Secondary eclipse is $\sim 180^\circ$ out of phase with the transit and is when the planet is occulted by the star, thereby shutting off the planet's contribution to the summed light. The approximate magnitude of this diminution varies significantly with wavelength, with the mid- to far-infrared being the most favorable bands. At 10-30 microns and in the Spitzer/IRAC bands from $3.6 \mu\text{m}$ to $8.0 \mu\text{m}$ this contrast was predicted to be $\sim 10^{-3}$ (Burrows, Sudarsky, & Hubeny 2003; Burrows 2005). This is near what has now been detected. In this paper, we customize to the TrES-1 and HD209458 systems the calculation of the planet-star flux-density ratio as a function of wavelength and compare the resulting theory with the Spitzer secondary eclipse data to draw conclusions about close-in EGP atmospheres. In §2, we summarize the new Spitzer data and in §3 we briefly describe our numerical techniques. Then, in §4 we present our results from $1 \mu\text{m}$ to $25 \mu\text{m}$ and wrap up in §5 with a discussion of our conclusions and the outstanding issues concerning irradiated EGPs that such eclipse data might address.

2. Summary of TrES-1 and HD209458b Data

The parameters of a transiting planetary system determine the inputs to a theoretical calculation of its spectrum and its planet-star flux-density ratio as a function of wavelength. Incident radiation at the planet’s surface is a function of the stellar flux density and the orbital distance, and the planet’s mass and radius determine the gravity of its atmosphere. For both TrES-1 and HD209458b, the interior flux (Burrows et al. 2000) is dwarfed by the irradiation effects for any reasonable system ages. Since we are not performing evolutionary calculations (Burrows et al. 2000; Burrows, Sudarsky, & Hubbard 2003 (BSH); Baraffe et al. 2003) in this paper, the system ages are not germane to the problem at hand, which is reproducing the observed planet-star flux-density ratios in the Spitzer bands. These ratios depend only on the stellar spectrum, the orbital distance, and the planet’s mass and radius, but not directly on age.

The K0V stellar primary of the transiting extrasolar giant planet TrES-1 is 157 ± 6 parsecs distant, has a T_{eff} of 5214 ± 23 K, a metallicity near solar ($[Fe/H] \sim 0$), a radius (R_*) of $0.83 \pm 0.03 R_\odot$, a mass (M_*) of $0.87 \pm 0.05 M_\odot$, and a bolometric luminosity (L_*) near half solar (Laughlin et al. 2005). The planet’s orbital and physical parameters are a semi-major axis (a) of 0.0393 AU, a period (P) of 3.030 days, a planet mass (M_p) of $0.729 \pm 0.036 M_J$ ² (Laughlin et al. 2005) or $0.76 \pm 0.05 M_J$ (Sozzetti et al. 2004), and a transit radius (BSH; Burrows et al. 2004) of approximately $1.08 \pm 0.05 R_J$ ³ (Alonso et al. 2004; Sozzetti et al. 2004; Laughlin et al. 2005).

The corresponding quantities for the F8V/G0V star HD209458 are 47.3 parsecs (Perryman 1997), $T_{\text{eff}} \sim 6000$ K, $[Fe/H] \sim 0$, $R_* = 1.2 \pm 0.1 R_\odot$, $M_* = 1.1 \pm 0.1 M_\odot$, and $L_* = 1.6 L_\odot$ (Henry et al. 2000; Charbonneau et al. 2000; Brown et al. 2001). The planet’s parameters are $a = 0.0468$ AU, $P = 3.524738$ days, $M_p = 0.69 \pm 0.02 M_J$, and $R_p = 1.32$ to $1.40 R_J$ (Henry et al. 2000; Charbonneau et al. 2000; Mazeh et al. 2000; Brown et al. 2001; Cody and Sasselov 2002; Fortney et al. 2003; Laughlin et al. 2005), with the lower value slightly more favored. Both TrES-1 and HD209458b have orbital inclinations near 90° and eccentricities near 0.

We see that the flux at the surface of TrES-1 is less than half that at the surface of HD209458b. Furthermore, the larger radius of HD209458b implies that it intercepts more than two times the radiative power. The former implies that the atmospheric temperature of HD209458b is likely to be higher than that of TrES-1, while the latter implies that HD209458b is bolometrically brighter. Nevertheless, as we show, their theoretical planet-

² M_J is the mass of Jupiter, $\sim 1.89914 \times 10^{30}$ gm

³ $R_J = 7.149 \times 10^4$ km, Jupiter’s radius

star ratios are not expected to be very different.

Prior to the recent measurements of the secondary eclipses that motivate this paper, Charbonneau et al. (2002) had uncovered evidence for the presence of sodium in the atmosphere of HD209458b from the different transit radii in and out of the Na-D line (see also Fortney et al. 2003). Similarly, Vidal-Madjar et al. (2003) had seen evidence for atomic hydrogen in a stellar-flux-induced planetary wind from HD209458b. The transit dip in Lyman- α is of such a magnitude ($\sim 15\%$) that the planetary material clearly extends beyond the Roche lobe, indicating planetary mass loss (Burrows & Lunine 1995; Lecavalier des Etangs et al. 2004). Other than these data, there had been no determinations to date of the composition of an extrasolar planet.

The new secondary eclipse data for TrES-1 (Charbonneau et al. 2005) and HD209458b (Deming et al. 2005) hint that this situation may be changing. TrES-1 shows eclipse depths (planet-star flux-density ratios) in the Spitzer/IRAC band centered at $4.5 \mu\text{m}$ of 0.00066 ± 0.00013 and in the Spitzer/IRAC band centered at $8.0 \mu\text{m}$ of 0.00225 ± 0.00036 (Charbonneau et al. 2005). HD209458b shows a corresponding ratio of 0.0026 ± 0.00045 in the Spitzer/MIPS band centered near $24 \mu\text{m}$ (Deming et al. 2005). These numbers are actually the ratios of detected electrons, an approximate substitute for the ratio of average flux densities in a given band. For flux density comparisons, one relies on flux calibrations that may not yet be robust, particularly given the significant differences between the spectra of a close-in EGP and a calibration star (e.g., Vega). Given this, in §4 we also provide theoretical bandpass-averaged detected-electron ratios.

Since the data from Charbonneau et al. (2005) and Deming et al. (2005) are but three of the ten potential data points (five bands \times two nearby transiting planets) we can expect using Spitzer, very-low-resolution spectra (but “spectra” nevertheless) of EGPs are anticipated soon that will provide compositional and atmospheric information of an unprecedented character.

3. Numerical Techniques, Databases, and Assumptions

The numerical tools we employ to derive the close-in planet’s spectrum during secondary eclipse are described in BSH and Burrows, Sudarsky, & Hubeny (2004), to which we refer the reader for further details. The spectral/atmosphere code COOLTLUSTY (Hubeny 1988; Hubeny and Lanz 1995; Sudarsky, Burrows, & Hubeny 2003) handles the effects of external irradiation using a first-order variant of the DFE (Discontinuous-Finite-Element) method. The incident flux is isotropically spread over the hemisphere of a given planar patch of

planetary “surface.” As described in BSH, to account in approximate fashion for the variation in incident flux with latitude when using a planar atmosphere code, as well as the possible day-night differences, we introduce the flux parameter f . A value of $f = 0.5$ assumes that there is little sharing of heat between the day and night sides of the EGP. A value of $f = 0.25$ assumes in the calculation of the T/P profile that the heat from irradiation is uniformly distributed by efficient winds over the entire sphere and that the infrared emissions are isotropic. For this study of the planet-star flux-density ratios of close-in EGPs, we use a fiducial value for f of 0.25, but we return to the issue of the proper choice of f in §5.

The emergent planetary spectra are calculated at 5000 wavelength points distributed logarithmically from 0.3 to 300 microns. The temperature-pressure profile in flux equilibrium is derived from $\sim 10^{-6}$ to $\sim 10^3$ bars. The spectral models for the stellar primaries (given a specific spectral subtype) come from Kurucz (1994). The molecular and atomic opacities are taken from the opacity library described in Burrows et al. (2001) and equilibrium compositions are derived using the updated thermochemical database of Burrows & Sharp (1999). Though the atmosphere is close to an ideal gas, the H/He equation of state of Saumon, Chabrier, & Van Horn (1995) that incorporates non-ideal effects is used.

4. Comparison of Theoretical Planet-Star Flux Ratios

Figure 2 depicts our theoretical planet-star flux-density ratios versus wavelength in the near- and mid-infrared for TrES-1 (magenta) and HD209458b (green). To derive these curves we have used the physical data for the planets and their primaries described in §2. Our baseline planet models have solar metallicity. The phase-averaged (Sudarsky, Burrows, & Hubeny 2003) flux ratios, but for $f = 0.25$ (§3; Sudarsky, Burrows, & Hubeny 2003; Burrows, Sudarsky, & Hubeny 2004), are given and have not been shifted in any way. Superposed are the new data at $24 \mu\text{m}$ for HD209458b (green) and at $4.5 \mu\text{m}$ and $8.0 \mu\text{m}$ for TrES-1 (gold). The vertical error bars are the quoted $1\text{-}\sigma$ ranges and the horizontal bars indicate the widths of the corresponding IRAC and MIPS bands. Also included in yellow are the four theoretical IRAC band-averaged fluxes for the TrES-1 model and in blue for the HD209458b model. These band averages are derived using the published transmission functions⁴, divided by frequency to obtain the theoretical ratio of detected electrons. Since the close-in EGP (this work) and stellar (Kurucz 1994) spectra are so flat at $24 \mu\text{m}$, a transmission band-averaged point is not shown (or needed) there.

Varying M_p , R_p , and R_* within the error bars alters the resulting planet-star flux-density

⁴See the IRAC web page at <http://ssc.spitzer.caltech.edu/IRAC/>

ratios only slightly. Similarly, and perhaps surprisingly, adding Fe and forsterite clouds does not shift the predictions in the Spitzer bands by an appreciable amount. Moreover, despite the more than a factor of two difference in the stellar flux at the planet, the predictions for the planet-star ratios for two such disparate close-in EGPs as TrES-1 and HD209458b are not very different. For TrES-1, raising or lowering the metallicity by a factor of three changes the flux ratios by less than $\sim 10\%$. Interestingly, however, changes in f and, by inference, day-night atmospheric differences and phase function effects can result in 25% to 50% deviations in the flux ratios of which one should take note.

Comparing our baseline models with data on Fig. 2, we can deduce several interesting things. First, the 24- μm data point is close to the predicted value, though for all three data points the theory slightly underestimates the data by a factor of ~ 1.5 -1.8, with the largest discrepancy being for the TrES-1 band at 8.0 μm . For HD209458b at 24 μm this deviation is only $\sim 1\sigma$. The high absolute values of the flux ratios imply that the close-in EGP atmospheres are indeed at high temperature, predicted for TrES-1 and HD209458b to be ~ 1500 K and ~ 1600 K, respectively, at a Rosseland depth of ~ 1 . Both atmospheres clearly span the temperature range 1000-2000 K. For TrES-1 at 8 μm , theory yields a brightness temperature (temperature at $\tau_\lambda = 2/3$) near 800-900 K, slightly lower than the ~ 1100 K crudely inferred from the data. At 4.5 μm , the theoretical brightness temperature of TrES-1 is ~ 750 -900 K (using $f = 0.25$), again slightly lower than the data might imply. However, care must be taken in estimating temperatures of any sort, and we will not, due to the hazards of extracting an “effective” or “equilibrium” temperature from these data, say much more about them. We do note, however, that given the radius of HD209458b and its general flux level, we expect that its bolometric luminosity is above $2 \times 10^{-5} L_\odot$. This is approaching the luminosity of a *star* $\sim 100\times$ the mass of HD209458b at the edge of the hydrogen-burning main sequence (Burrows et al. 2001).

In Fig. 2, there is a hint of the presence of H_2O , since it is expected to suppress flux between 4 μm and 10 μm . This is shortward of the predicted 10- μm peak in planet-star flux-density ratio, which is due to water’s relative abundance and the strength of its absorption bands in that wavelength range. Figure 3 demonstrates this by comparing H_2O , CH_4 , and CO opacities per molecule from 0.5 to 10 microns. Without H_2O , the fluxes in the IRAC bands would be much higher than the fluxes in the mid-infrared. Hence, a comparison of the TrES-1 and HD209458b data at 4.5/8.0 μm and 24 μm suggests, but does not prove, the presence of water. As Fig. 3 implies, seeing the expected slope between the 5.8- μm and 8.0- μm bands and the rise from 4.5 μm to 3.6 μm would be more revealing in this regard and is a prediction of our theory. Furthermore, the relative strength of 24- μm MIPS flux ratio in comparison with the 3.6- μm , 4.5- μm , and 5.8- μm IRAC channel ratios is another prediction of the models, as is the closeness of the 8.0- μm and 24- μm ratios. The latter seems borne

out by the data, though these data are for two different objects.

Nevertheless, the models have difficulty fitting the depth of the $4.5\text{-}\mu\text{m}$ feature in TrES-1. This feature coincides with the strong CO absorption predicted to be a signature of hot EGP atmospheres (Fig. 3; Sudarsky, Burrows, & Hubeny 2003; Burrows, Sudarsky, & Hubeny 2004; Burrows 2005), but is shallower than expected and $\sim 2\text{-}\sigma$ discrepant. The data are in fact the band-averaged flux-density ratios of the detected electrons. As such, the larger fluxes on either side of the trough theoretically centered close to $4.5\text{ }\mu\text{m}$ contribute planet flux to the detected band. As a result, the yellow dot that represents this integrated band contribution is a weak function of CO abundance. In fact, a CO abundance $100\times$ larger than expected in chemical equilibrium lowers this flux ratio at $4.5\text{ }\mu\text{m}$ by only $\sim 25\%$. Therefore, while the $4.5\text{-}\mu\text{m}$ data point for TrES-1 implies that CO has been detected, the exact fit is problematic. More data and further attention to calibration are called for. However, as we have indicated and discuss in §5, the contrast between theory and measurement at all data points may be a signature of day-night infrared flux asymmetry. The close-in planets may not be radiating heat energy isotropically (as is assumed when using $f = 0.25$), a not-unexpected result (Guillot & Showman 2002).

5. Discussion

We predict that both the $3.6\text{-}\mu\text{m}$ and the $5.8\text{-}\mu\text{m}$ flux ratios will be higher than the $4.5\text{-}\mu\text{m}$ ratio by at least 50% and that the pattern of the yellow and blue dots on Fig. 2 will be realized. We also predict that the $24\text{-}\mu\text{m}$ flux ratio for TrES-1 will be similar to that seen for HD209458b (Deming et al. 2005). However, while the close correspondence of the measured and theoretical fluxes depicted on Fig. 2 is striking, it is not perfect. What could explain the differences? One major uncertainty is the day-night atmospheric profile difference. HD209458b and TrES-1 are close enough to their primaries to be in synchronous rotation. Therefore, they show the same hemisphere to the star at all times. It is the zonal winds, atmospheric circulation currents, and jet streams (Menou et al. 2002; Guillot & Showman 2002; Showman & Guillot 2002; Cho et al. 2003; Burkert et al. 2005) that advect heat from the day to the night sides, thereby affecting the atmospheric temperature structure as a function of longitude. How much of the stellar radiation goes to heating the day side (visible just before and after the secondary eclipse) and how much is transported by mass motion away from the day side to heat the night side? This question remains unresolved, but directly impinges upon the planet-star flux-density ratios in the infrared measured during secondary eclipses.

The f factor we use for our fiducial model (0.25) is tailored to distribute heat over

the entire planet, on both the day and the night sides. The three data points depicted in Fig. 2 are all factors of ~ 1.5 - 1.8 above the $f = 0.25$ theory curves. This implies that the planet’s radiation is predominantly radiated by the day side and that its emissions are forward-beamed. This is not entirely unexpected in the optical, but seems to be the case in the mid-infrared as well. The implication of the new secondary eclipse data at $24\ \mu\text{m}$ and $8\ \mu\text{m}$ may be that we are seeing indirect signs of an asymmetry in the day-night heating and temperature profiles, with the day side hotter than the night side by at least $500\ \text{K}$. This estimate is based on the mid-infrared “excesses” seen in Fig. 2, on the possible model variations, and on the measurement errors. However, the confirmation of such a conclusion awaits more detailed multi-dimensional general circulation models with correct transport, next-generation models of the wavelength-dependent phase functions of close-in EGPs (Sudarsky, Burrows, Hubeny, & Li 2005), and, most importantly, additional data.

It has long been suggested, and recently articulated (Cooper & Showman 2005), that due to winds the sub-stellar point of an irradiated close-in EGP may not be the hottest spot. Advection would introduce a lag even for circular orbits between the planet’s ephemeris and its light curve (the light curve would lead). Cooper & Showman (2005) estimate that the lead could be as much as 60° and could amount to a 20% brightness shift in the value at superior conjunction. A 20% decrement is not enough to close the modest apparent gap between our theory and the $24\text{-}\mu\text{m}$ data for HD209458b, and is not of the correct sign. However, the concept of a shift in the light curve deserves further scrutiny.

Charbonneau et al. (2005) estimate a Bond albedo (A) for TrES-1 of 0.31 ± 0.14 . However, one should be very cautious using these new data to infer temperatures and reflection coefficients. Not only is the reradiation not expected to be isotropic off the planet, but the atmospheres are not black bodies. While one can distinguish hot atmospheres (1000 - $2000\ \text{K}$) from cooler atmospheres (500 - $1000\ \text{K}$), the data and theory are not yet adequate to allow these TrES-1 data to strongly constrain A . However, if A were in the 0.31 ± 0.14 range, this would imply that there is a cloud of non-trivial optical depth in the upper layers of TrES-1, putting it into the “Class V” category of EGPs, rather than the “Class IV” category (Sudarsky, Burrows, & Pinto 2000). The latter, due to strong absorption bands and little Rayleigh scattering, have very low Bond albedos (below 0.05). Our models for TrES-1 would favor the low-albedo Class IV category for TrES-1 and the higher-albedo Class V category for HD209458b, but we feel it is premature to conclude anything definitive about albedos at this stage (other than that they can not be very high and that the close-in EGPs can not be highly reflective).

In this paper, we have calculated planet-star flux-density ratios versus wavelength, focussing on the near- and mid-infrared out to $25\ \mu\text{m}$ and the irradiated close-in extrasolar

giant planets TrES-1 and HD209458b, and have compared our theory with the recent secondary eclipse data from Charbonneau et al. (2005) and Deming et al. (2005). We have inferred the presence of carbon monoxide, and perhaps water, in the atmosphere of TrES-1 and have determined that both atmospheres are hot (~ 1000 - 2000 K). We have explored the effects of varying the metallicity, M_p , R_p , and R_* , the latter three within the stated error bars, and find our predictions for the planet-star flux-density ratios to be robust. However, more work is required to understand the apparent shallowness of the TrES-1 $4.5\text{-}\mu\text{m}$ trough. (Non-LTE and non-equilibrium effects in the chemistry may be worth exploring, as well as the consequences of possible stratospheric temperature inversions (Smith & Hunten 1990).) However, we suggest that the data (particularly at 8 and 24 microns) indicate we are beginning to constrain the degree of anisotropy in the temperature profile of a close-in EGP (the day-night contrast) and in the angular dependence of its emission. Our preliminary conclusion is that the slight systematic differences seen in Fig. 2 between the phase-averaged theory and all three new measurements may be explained in part by an infrared-brighter, hotter day side. This raises the intriguing possibility that additional and more precise secondary eclipse data for these transiting EGPs could shed light on their global meteorology. Be that as it may, these secondary eclipse data are opening a new chapter in the accelerating study of extrasolar planets and emphasize that knowledge of a unique character is generated when new capabilities emerge.

We thank Christopher Sharp, Bill Hubbard, and Drew Milsom for useful discussions during the course of this investigation and Dave Charbonneau for an advanced look at the TrES-1 secondary eclipse data. This study was supported in part by NASA grants NNG04GL22G and NAG5-13775. This material is based upon work supported by the National Aeronautics and Space Administration through the NASA Astrobiology Institute under Cooperative Agreement No. CAN-02-OSS-02 issued through the Office of Space Science.

REFERENCES

- Allard, F., Baraffe, I., Chabrier, G., Barman, T.S., & Hauschildt, P.H. 2003, in “Scientific Frontiers in Research on Extrasolar Planets,” ASP Conf. Series vol. 28 (PASP v.294), eds. D. Deming & S. Seager, p. 483
- Alonso, R. et al. 2004, ApJ, 613, L153
- Baraffe, I., Chabrier, G., Barman, T.S., Allard, F., & Hauschildt, P.H. 2003, A&A, 402, 701

- Bouchy, F., Pont, F., Santos, F.C., Melo, C., Mayor, M., Queloz, D., & Udry, S. 2004, astro-ph/0404264
- Brown, T. M., Charbonneau, D., Gilliland, R.L., Noyes, R.W., & Burrows, A. 2001, ApJ, 552, 699
- Burkert, A., Lin, D.N.C., Bodenheimer, P., Jones, C., & Yorke, H. 2005, ApJ, 618, 512
- Burrows, A. & Lunine, J.I. 1995, Nature, 378, 333
- Burrows, A., Marley, M., Hubbard, W. B., Lunine, J. I., Guillot, T., Saumon, D., Freedman, R., Sudarsky, D., & Sharp, C. 1997, ApJ, 491, 856
- Burrows, A. & Sharp, C. M. 1999, ApJ, 512, 843
- Burrows, A., Guillot, T., Hubbard, W. B., Marley, M. S., Saumon, D., Lunine, J. I., & Sudarsky, D. 2000, ApJ, 534, 97
- Burrows, A., Hubbard, W.B., Lunine, J.I., and Liebert, J. 2001, Rev. Mod. Phys., 73, 719
- Burrows, A., Sudarsky, & Hubbard, W.B. 2003, ApJ, 594, 545 (BSH)
- Burrows, A., Sudarsky, D., & Hubeny, I. 2003, published in the proceedings of the 14th Annual Astrophysics Conference in Maryland “The Search for Other Worlds,” eds. S. Holt and D. Deming, (AIP Conference Proceedings), held in College Park, MD, October 13-14, 2003, p. 143.
- Burrows, A., Sudarsky, D., & Hubeny, I. 2004, ApJ, 609, 407
- Burrows, A., Hubeny, I., Hubbard, W.B., Sudarsky, D., & Fortney, J.J. 2004 ApJ, 610, L53
- Burrows, A. 2005, Nature, 433, 261
- Charbonneau, D., Brown, T. M., Latham, D. W., & Mayor, M. 2000, ApJ, 529, L45
- Charbonneau, D., Brown, T. M., Noyes, R. W., & Gilliland, R. L. 2002, ApJ, 568, 377
- Charbonneau, D. et al. 2005, accepted to ApJ
- Cho, J. Y-K., Menou, K., Hansen, B. M. S., & Seager, S. 2003, ApJ, 587, L117
- Cody, A. M. & Sasselov, D. D. 2002, ApJ, 569, 451
- Cooper, C.S. & Showman, A.P. 2005, submitted to ApJ, (astro-ph/0502476)

- Deming, D., Seager, S., Richardson, L.J., & Harrington, J., 2005, accepted to Nature
- Fortney, J.J., Sudarsky, D., Hubeny, I., Cooper, C.S., Hubbard, W.B., Burrows, A., & Lunine, J.I. 2003, ApJ, 589, 615
- Guillot, T., Burrows, A., Hubbard, W. B., Lunine, J. I., & Saumon, D. 1996, ApJ, 459, 35
- Guillot, T. & Showman, A. P. 2002, A&A, 385, 156
- Henry, G., Marcy, G. W., Butler, R. P., & Vogt, S. S. 2000, ApJ, 529, L41
- Hubeny, I. 1988, Computer Physics Comm., 52, 103
- Hubeny, I. & Lanz, T. 1995, ApJ, 439, 875
- Konacki, M., Torres, G., Jha, S., & Sasselov, D. 2003, Nature, 421, 507
- Konacki, M., Torres, G., Sasselov, D., & Jha, S. 2003, ApJ, 597, 1076
- Konacki, M., et al. 2004, ApJ, 609, L37 (astro-ph/0404541)
- Kurucz, R. 1994, *Kurucz CD-ROM No. 19*, (Cambridge: Smithsonian Astrophysical Observatory)
- Laughlin, G., Wolf, A., Vanmunster, T., Bodenheimer, P., Fischer, D., Marcy, G., Butler, P., & Vogt, S. 2005, preprint
- Lecavelier des Etangs, A. et al. 2004, A&A, 418, L1
- Marcy, G.W. & Butler, R.P. 1996, ApJ, 464, L147
- Marcy, G.W. & Butler, R.P. 1998, ARA&A, 36, 57
- Marcy, G.W., W. Cochran, W., & Mayor, M. 2000, in *Protostars and Planets IV*, ed. V. Mannings, A.P. Boss, and S.S. Russell (Tucson: The University of Arizona Press), p. 1285-1311
- Mayor, M. & Queloz, D. 1995, Nature, 378, 355
- Mazeh, T., Naef, D., Torres, G., et al. 2000, ApJ, 532, L55
- Menou, K, Cho, J. Y-K., Hansen, B. M. S., & Seager, S. 2003, ApJ, 587, L113.
- Perryman, M.A.C. 1997, *The Hipparcos and Tycho Catalogues* (ESA SP-1200, Noordwijk:ESA)

- Pont, F., Bouchy, F., Queloz, D., Santos, N. C., Melo, C., Mayor, M., & Udry, S. 2004, *A&A*, 426, L15
- Saumon, D., Chabrier, G., & Van Horn, H. 1995, *ApJS*, 99, 713
- Sasselov, D. 2003, *ApJ*, 596, 1327
- Showman, A. P. & Guillot, T. 2002, *A&A*, 385, 166
- Smith, G. R. & Hunten, D. M. 1990, *Rev. Geophys.*, 28, 117
- Sozzetti, A. et al. 2004, *ApJ*, 616, L167 (astro-ph/0410483)
- Sudarsky, D., Burrows, A., & Pinto, P. 2000, *ApJ*, 538, 885
- Sudarsky, D., Burrows, A., & Hubeny, I. 2003, *ApJ*, 588, 1121
- Sudarsky, D., Burrows, A., Hubeny, I., & Li, A. 2005, accepted to *ApJ*(astro-ph/0503187)
- Torres, G., Konacki, M., Sasselov, D., & Jha, S. 2005, *ApJ*, 619, 558 (astro-ph/0310114)
- Vidal-Madjar, A., Lecavelier des Etangs, A., Désert, J.-M., Ballester, G.E., Ferlet, R., Hébrard, G., & Mayor, M. 2003, *Nature*, 422, 143

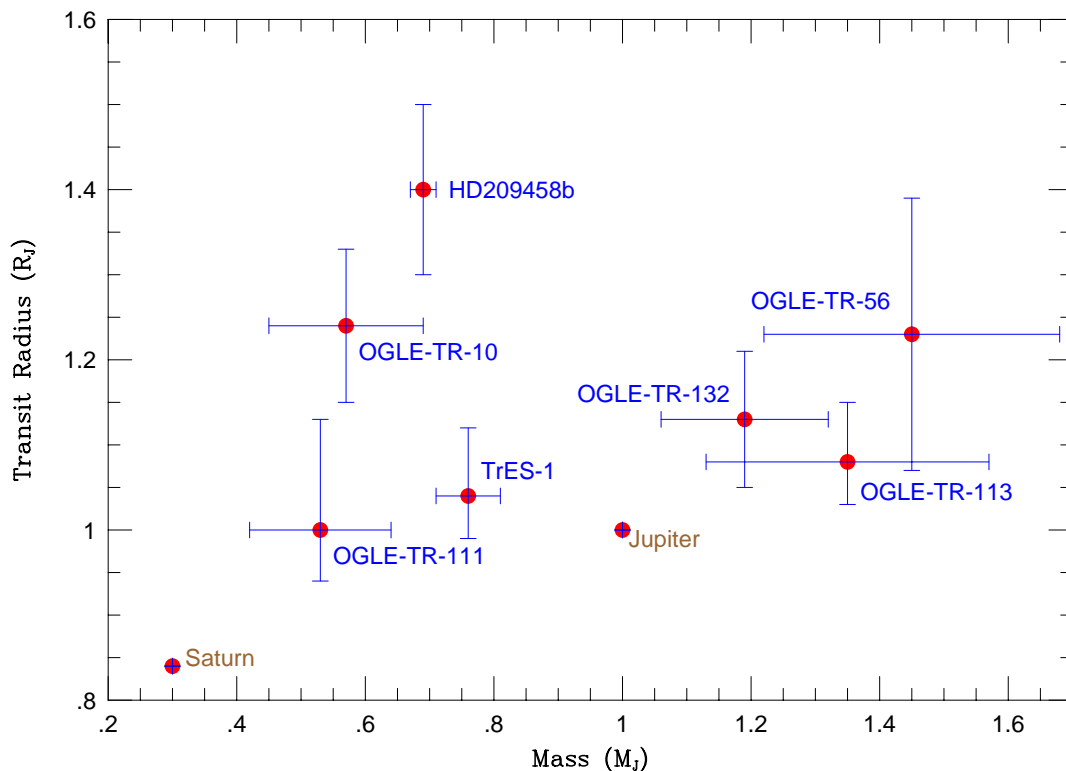


Fig. 1.— Transit radii (in units of Jupiter’s radius) with error bars versus planet mass with error bars (in units of Jupiter’s mass) for the seven EGPs currently seen to transit their primaries. The positions of Jupiter and Saturn themselves are included for comparison. Note that HD209458b is the largest transiting EGP (Mazeh et al. 2000; Brown et al. 2001; Cody and Sasselov 2002) and, as such, is an outlier, though most of these irradiated EGPs are clearly larger than Jupiter. An extended transit radius is a known consequence of stellar irradiation (Guillot et al. 1996; Burrows et al. 2000; Burrows, Sudarsky, & Hubbard 2003; Baraffe et al. 2003; Chabrier et al. 2004; Burrows et al. 2004).

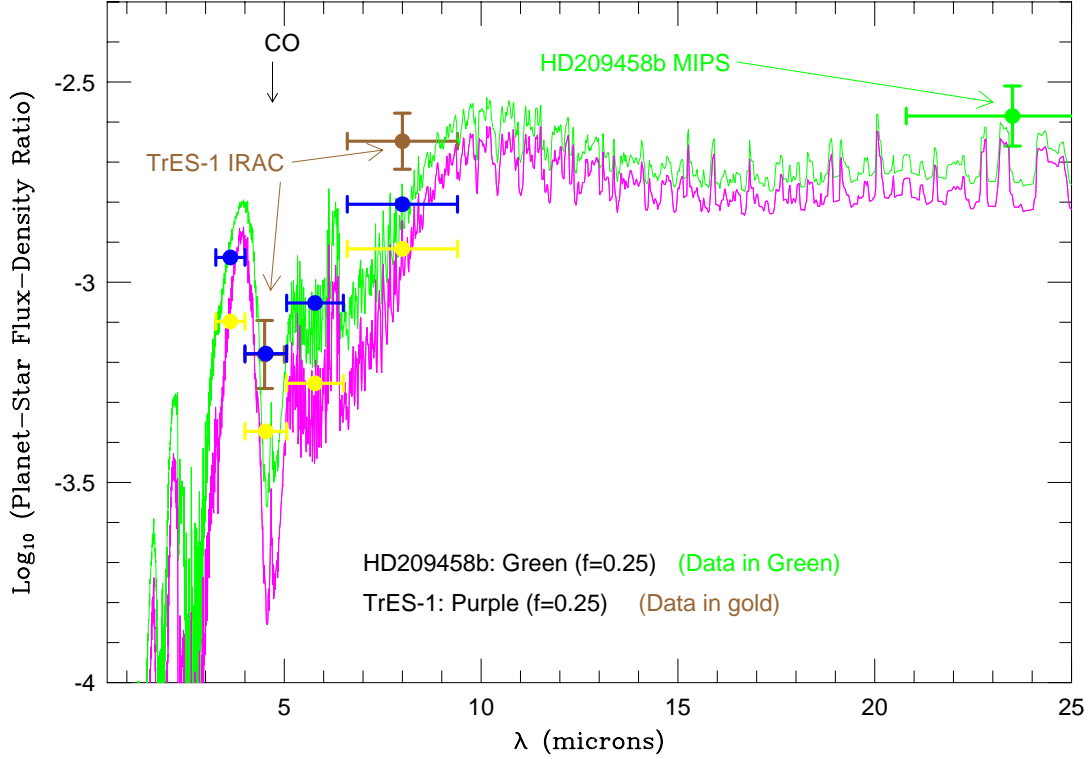


Fig. 2.— The logarithm base ten of the planet-to-star flux-density ratio as a function of wavelength (λ , in microns) for our baseline models of TrES-1 and HD209458b (for $f = 0.25$). The model for TrES-1 is purple and that for HD209458b is green. Superposed are the secondary eclipse data: the gold dots with corresponding error bars are the TrES-1 Spitzer/IRAC data from Charbonneau et al. (2005), while the green dot with error bars is the HD209458b Spitzer/MIPS 24- μm datum from Deming et al. (2005). Also included are the band-averaged detected-electron/“flux” ratios for the TrES-1 (yellow) and HD209458b (blue) models in the four IRAC bands. Note that coincidentally the blue dot at 4.5 μm overlaps the gold TRES-1 data point. The position of the strong CO absorption feature at $\sim 4.67 \mu\text{m}$ is indicated and clearly coincides with the $\sim 4.5 \mu\text{m}$ IRAC band flux. See text for a discussion and details.

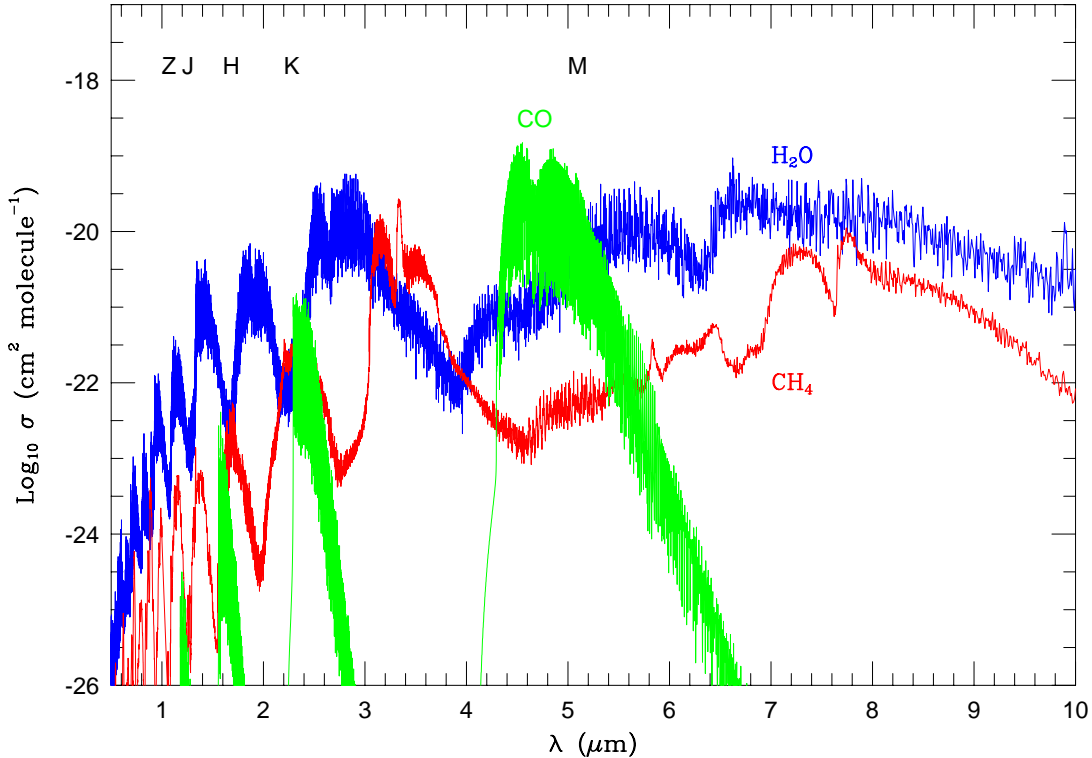


Fig. 3.— The logarithm base ten of the absorption cross section per molecule (in cm^2) versus wavelength (in microns) from $0.5 \mu\text{m}$ to $10 \mu\text{m}$ for water (H_2O), carbon monoxide (CO), and methane (CH_4). These numbers are not weighted by abundance. A comparison with Fig. 2 clearly shows that CO is probably present in TrES-1 and that water helps shape the planet-star flux-density ratio in the 4 to 9 micron spectral region. Shown also are the positions of various standard photometric bands (Z , J , H , K , M). This figure, in conjunction with Fig. 2, demonstrates that if CH_4 is present in abundance in either HD209458b or TrES-1 then the $3.6\text{-}\mu\text{m}$ IRAC band will test this. However, our expectation for these close-in EGPs is that CH_4 will not be in evidence. When data for all four IRAC bands are available, we should be able to verify definitively the presence of water vapor in the atmosphere of an extrasolar giant planet, though by the absolute level at $8.0 \mu\text{m}$ of the TrES-1 flux in Fig. 2 the presence of water already seems likely. See text for further discussion.